Indian Journal of Engineering & Materials Sciences
Vol. 31, October 2024, pp. 699-713
DOI: 10.56042/ijems.v31i5.11134

A parametric study of interlayer incorporated friction stir welded Al/Cu and its effect on microstructure and mechanical properties

Viresh Payak*, Jawahar Paulraj, Barnik Saha Roy, Smrity Choudhury & Rahul Das
Mechanical Engineering Department, NIT Agartala, Agartala Tripura 799 046, India

Received: 14 May 2024; accepted: 30 August 2024

This study examines the influence of various parameters on the microstructural and mechanical characteristics of friction stir-welded 3 mm thick AA6101/C11000 dissimilar joints with a hybrid interlayer consisting of Ag and Zn. Using scanning electron microscopy and energy-dispersive X-ray spectroscopy, this study provides valuable insights into the microstructural examination of joints. This study identified the optimal weld parameters to achieve a sound weld with good mechanical properties in AA6101/C11000 joints. As there was a lack of optimal weld parameters for the friction stir welding of AA6101/C11000 joints using the interlayer approach, the study carefully derived the optimal weld parameters for achieving sound welds and optimal mechanical properties. The study found that different traverse speeds (0.75 mm/s, 1.25 mm/s, 2.25 mm/s) had varying tensile strengths, which were influenced by the thickness and brittleness of the intermetallic layer. The rotational speed, ranging from 800 to 1800 rpm, also had an impact on intermetallic formation. Higher rotational speeds resulted in thicker intermetallic layers and reduced the tensile strength. The study found that a sound weld surface was achieved at 1200 rpm, which allowed for proper diffusion, controlled intermetallic formation, and solid-solution phase development, resulting in the highest tensile strength. The microstructure of the joint revealed a composite-like structure with dispersed Cu, Ag, and Zn particles in the Al matrix. The nugget zone displayed several phases, including Al-Zn solid solution,$Al_{4.2}Cu_{3.2}Zn_{0.7}$, (Ag-Cu) rich, and Ag_2Al, which contributed to the highest tensile strength (156.19±10.08 MPa). The optimal joint strength and efficiency were observed at 1200 rpm, emphasizing the importance of rotational speed. At 1200 rpm, the fracture surface exhibited dimples, indicating ductile fracture. The incorporation of the Ag and Zn interlayers helped reduce the formation of highly brittle intermetallic compounds (IMCs), promoting less harmful phases and contributing to ductile fracture behaviour and the highest tensile strength.

Keywords: Aluminium, Copper, Friction stir welding, Microstructure, Mechanical properties, Parametric study

1 Introduction

Dissimilar materials joining has emerged as a significant engineering strategy, offering various advantages such as lightweight design, hybrid properties, cost efficiency, enhanced structural integrity, improved performance, etc.[1-4]. Composite structures made from aluminium and copper alloys are particularly well-suited for applications in chemical, transportation, energy, aviation, and electronics industries. Consequently, the dissimilar joining of aluminium and copper has gathered significant attention, leading to rapid advancements in dissimilar materials joining technology [5-10].

The challenge in joining Al-Cu arises from differences in its physical, mechanical, and chemical properties, leading to the formation of undesirable brittle IMCs[11, 12]. Traditional welding methods, such as fusion welding, have been used to create Al-Cu joints, but they can result in issues such as solidification cracking, oxidation, and the formation of brittle IMCs, which negatively affect the mechanical properties of welded structures [13, 14]. Friction stir welding (FSW), a solid-state process, has emerged as a promising solution for joining dissimilar alloys such as aluminium and copper. Compared with fusion welding, FSW reduces the formation of IMCs because joining occurs in the solid state [15]. Nevertheless, researchers have still detected various IMCs in Al-Cu joints, including Al_2Cu and Al_4Cu_9 in pure Cu /AA6082-T6 joints [16] and AA6000-T6/pure Cu joints [17], as well as AlCu in A1100H24-Cu FSW welds [18].

FSW is a technology that has been proven useful for joining dissimilar materials despite the challenges it presents. Unlike traditional fusion welding techniques, FSW offers several advantages. Nevertheless, the strength of friction stir welds is hindered by the brittleness of IMCs. Studies have highlighted that the thickness of the IMC reaction

*Corresponding author: (E-mail- vireshpayak55@gmail.com)

layer significantly influences the interfacial strength of welds. Essentially, the strength of the joint decreases as the thickness of the IMC layer increases.

Researchers have suggested improving the properties of FSWed Al-Cu joints by managing the thickness of IMCs. It was noted that the thickness can be controlled by adjusting the process parameters to a certain extent. Surprisingly, it was pointed out that in the last decade, the thickness of the IMCs has been reduced, and the type of IMC formation has been controlled by introducing third-phase metal as interlayer [19, 20]. It was very much fascinating to see that the introduction of Zn as interlayer has led to the formation of IMCs $CuZn_5$, CuZn, Cu_5Zn_8 [21-23] with Cu, which is less detrimental and less brittle than IMCs formed without Zn interlayers AlCu, Al_2Cu, Al_2Cu_3, Al_3Cu_4, and Al_4Cu_9 [24-27]. Similarly it was also noted that incorporation of Ag as interlayer in FSWed Al-Cu joint has led to the formation of IMCs Ag_2Al [28] with Al in the nugget zone which is also less brittle.

Significantly, it was noted that Zn predominantly forms IMC with Cu, and Ag forms IMC with Al, which are comparatively less brittle. However, other intermetallics of Al-Cu such as Al_2Cu, Al_4Cu_9 were also noted [15, 28-30]. It provides a conceptual precipitation that when Ag & Zn is being used together as interlayer the formation of highly brittle intermetallics between Al-Cu may be completely removed. In our earlier research FSWed Al-Cu joints has been carried out using hybrid Ag & Zn as interlayer in controlled parameters observed the formation $CuZn_5$ and Ag_2Al [31] only as intermetallics which is less brittle than Al_2Cu, Al_4Cu_9. This finding has motivated us to study the influence of Ag & Zn as interlayers on mechanical characteristics of FSWed Al-Cu joints experimentally. The impact of rotational speed and traverse speed on mechanical strength was analysed, and the optimum was reported experimentally in this manuscript.

2 Materials and Methods

This research utilized 6101 Aluminium alloy (AA6101) and Copper (C11000) plates as workpiece materials. These plates have dimensions of length 150 mm, breadth 60 mm and thickness 3 mm, and are friction stir butt-welded to achieve a sound joint. Table 1 provides the chemical composition of the weight percentages of both Al and Cu, while Table 2 outlines the mechanical properties. To prepare the welding surfaces of the parent materials (Al and Cu) for the welding process and ensure joint quality, abrasive paper was used for grinding. Subsequently, the surfaces were degreased with acetone to remove the oil, oxide film, and other impurities. Fig. 1 shows a schematic view of the Al/Cu plate setup with the hybrid interlayer used in this study.

The FSW process involves the movement of deformed material from the retreating side (RS) to the advancing side (AS). In this study (as shown in Fig. 2), the Cu and Al plates were strategically placed on the AS and RS, respectively. This placement was based on the observation by researchers that

Table 1 — Chemical composition (wt. %) of base materials.

	Mg	Si	Al	Cu
AA 6101	0.6	0.5	98.9	
C11000				99.9

Table 2 — Mechanical properties of base materials.

Materials	Density	Tensile Strength	Melting Point
AA 6101	2.7 (g/cm^3)	197 MPa	588 °C
C11000	8.89 (g/cm^3)	220 MPa	1083 °C

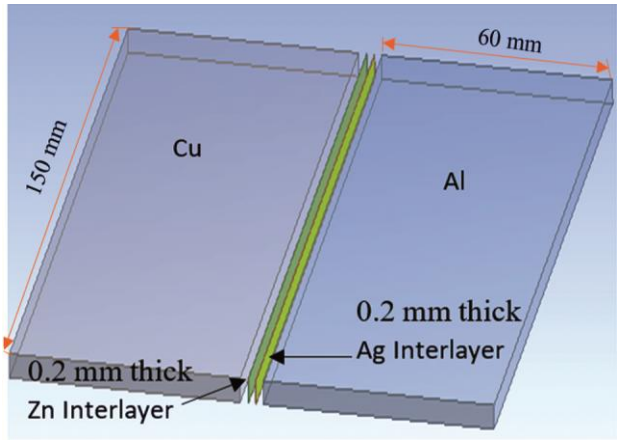

Fig. 1 — The arrangements for friction stir welding (FSW) of Al/Cu.

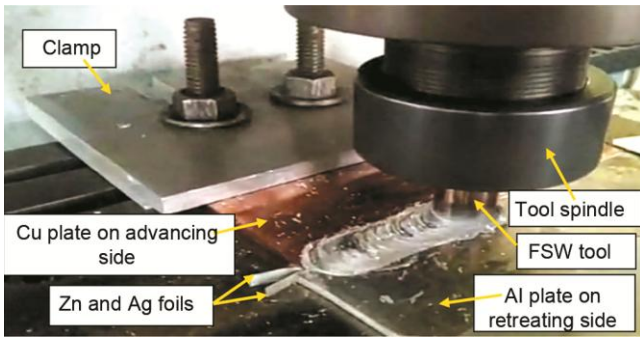

Fig. 2 — Schematic of dissimilar joining of Al and Cu FSW.

placing the Cu on the AS resulted in superior weld quality [32-34].

Additionally, the advancing side in FSW generates more heat. To achieve optimal mechanical properties for the dissimilar joint, a tool offset of 1 mm towards the Al side was taken into account. A plane tapered pin tool made of H13 tool steel with a shoulder diameter of 18 mm, a height of 2.7 mm, and root and tip diameters of 6 mm and 4 mm, respectively, was used (refer to Fig. 3). All welding experiments were carried out using a CNC 3-ton FSW machine (WS005, ETA Technology, Bangalore).

A series of trial experiments (Table 3) utilizing a trial-and-error approach were carried out to identify the suitable range of TRS, TTS and tilt angle for the final welding process. The TRS ranged from 800 rpm to 1600 rpm based on the trial experiments, as welds beyond this lower and upper limit exhibited defects. The lower limit for TTS was set at 0.75 mm/sec because, below this limit, there is a tendency for the formation of very hard IMCs at extremely TTS [35-37]. The highest TTS value obtained from the trial experiments was 2.25 mm/sec, beyond which defective welds were observed. The impact of tilt angle variation on dissimilar aluminium-to-copper joining has not been widely explored. To address this gap, trial experiments were conducted, systematically varying the tilt angle from 1º to 3º while maintaining constant rotational speed and traverse speed. It was observed that welds at a 2º tilt angle were free from defects. The tilting of the tool generates high frictional forces, enhancing the stirring between the workpiece and the tool. This results in improved interfacial material flow from the AS to the RS of the joined samples.

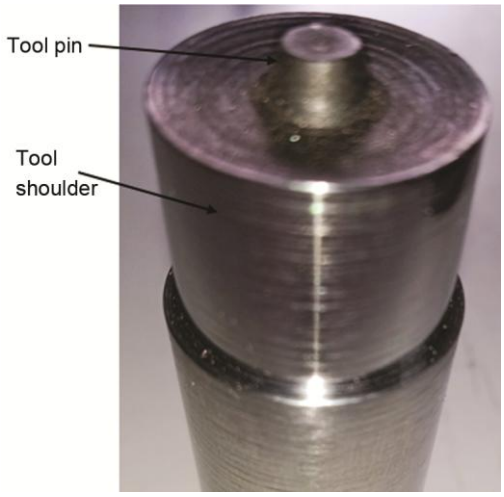

Fig. 3 — Tool with taper pin.

Table 3 — The chosen FSW parameters for Al6101/C11000 Joints.

Experiment Number	Rotational Speed (rpm)	Traverse Speed (mm/s)	Tilt Angle
J_1	800	1.25	1°
J_2	800	1.25	2°
J_3	800	1.25	3°
J_4	800	0.75	2°
J_5	800	2.25	2°
J_6	1000	1.25	2°
J_7	1200	1.25	2°
J_8	1400	1.25	2°
J_9	1600	1.25	2°
J_{10}	1800	1.25	2°

The welded plates considered for visual inspection to identify any defects or irregularities, and the details of all the welded joints are presented in Table 4. The samples for testing were obtained by cutting the transverse section of the welded plate. Subsequently, the metallographic samples were polished using abrasive paper and colloidal silica. The prepared samples were then analysed using scanning electron microscopy (SEM, CARL ZEISS EVO 50) and subjected to energy-dispersive X-ray spectroscopy (EDS).

The mechanical characteristics of the Al/Cu joints were assessed via tensile strength tests and examination of the fractured surfaces. Tensile tests were conducted using an Instron-1195 universal testing machine with a consistent cross-head speed of 0.5 mm/min at room temperature. The specimens were prepared according to the ASTM E8 standard, and three samples were tested for each welding condition, as shown in Fig. 4.

3 Results and Discussion

The obtained results were examined to understand the impact of various process factors, including traverse speed, rotational speed, and tool tilt angle, on the friction stir welding of Al6101/Hybrid interlayer (Ag-Zn)/C11000.

3.1 Surface appearance of the joints

Table 4 shows the surface characteristics of the Al/Cu butt joints, revealing the successful creation of defect-free friction stir-welded Al/Cu joints for J_2, J_6, J_7, J_8, and J_9 in this study. These joints displayed even and seamless weld surfaces, free from cracks or tunnels, indicating adequate heat input for proper material flow in friction-stir-welded joints.

Table 4 — The visual appearance of the weld surfaces and the cross-sectional structure of all the created joints.

Joints	Weld surface appearance	Cross-sectional macrostructure	Remarks
J_1		Broke while sample preparation	Lack of penetration and proper mixing due to insufficient tilt angle
J_2		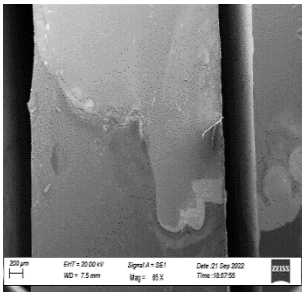	No defects
J_3		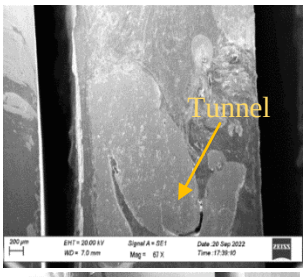	Amount of heat and pressure may not be adequate due to incorrect combination of parameters
J_4	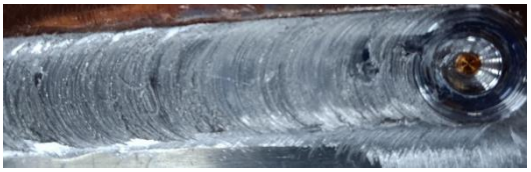	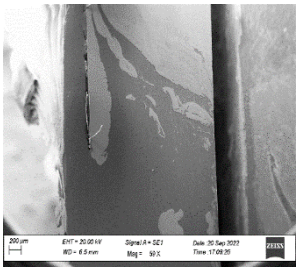	Amount of heat and pressure may not be adequate due to incorrect combination of parameters
J_5		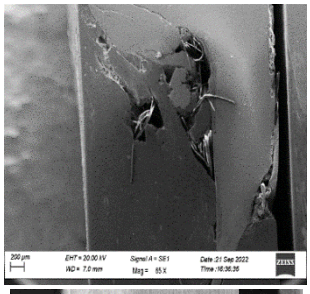	Lack of heat and pressure due to inappropriate parametric combination generates voids which continue through the entire weld
J_6	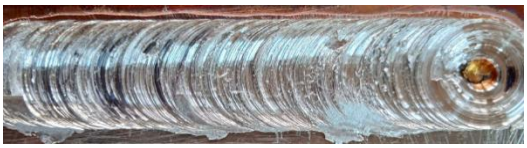	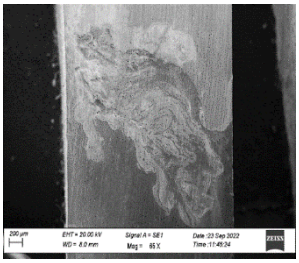	No defects

(*Contd.*)

Table 4 — The visual appearance of the weld surfaces and the cross-sectional structure of all the created joints. (*Contd.*)

Joints	Weld surface appearance	Cross-sectional macrostructure	Remarks
J_7	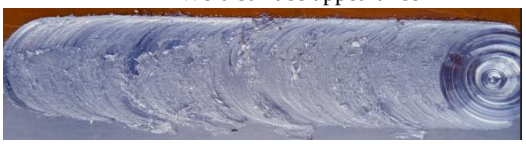	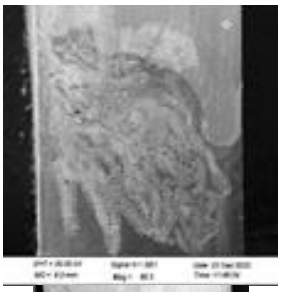	No defects
J_8		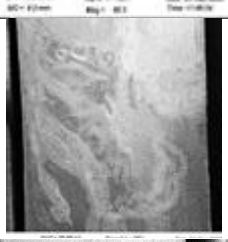	No defects
J_9		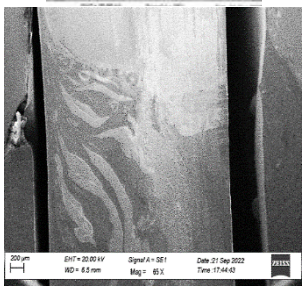	No defects
J_{10}		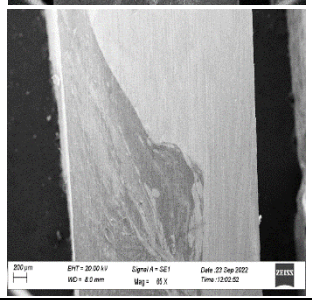	No defects

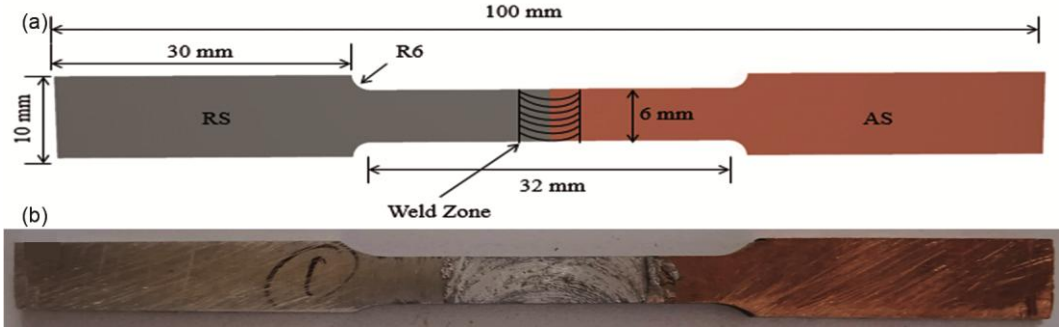

Fig. 4 — (a) Dimensions of prepared specimens for tensile test, and (b) Tensile test specimen.

Moreover, some flashes were observed in the joints' appearance, which could be attributed to the use of higher rotational speed and lower welding speed, leading to severe plastic deformation and the formation of flash [38].

3.2 Joints macrographs and microstructures

Table 4 illustrates two different interaction patterns, as outlined by Galvao et al. in their study [39]. These patterns are evident in the form of intercalated lamellar structures in J_6, composite-like structures in

J_7, and a combination of intercalated lamellar structures and composite-like structures in J_8&J_9. It is important to note that the aluminum and copper surfaces display irregular characteristics owing to mechanical stirring, which can result in the removal of copper particles from the base material. The composite-like structure in J_7 shows homogeneous distribution of copper particles throughout the stir zone, despite variations in their morphologies across the welding processes. This variation may result in the development of interfacial reaction layers with diverse configurations within the welds. The miscibility level, intercalation of lamellar structures, and distribution of Cu and interlayer particles in the stir zone exhibited distinct characteristics. Such diverse behaviours are expected in dissimilar Al/Cu FSW welds, as previously suggested [33, 40-42].

The microstructural characteristics of Al/Cu joints in Fig. 5 align with those identified defect-free in Table 4. As demonstrated in Fig. 5, the material flow within the stir zone presents distinct patterns, even when the welded materials are identical in all instances. The dissimilarity is mainly attributed to the intermittent plastic deformation resulting from variations in flow stress between aluminium and copper, which are caused by different FSW process parameters [43]. In all examined joints, copper (Cu) is conspicuously present in diverse shapes and sizes, accompanied by extensively distributed interlayer particles within the nugget zones (NZ). This distribution results in a structure that resembles a particle-reinforced composite-like configuration, consistent with findings reported in prior studies [13, 31, 40, 44]. Additionally, the stirred region and

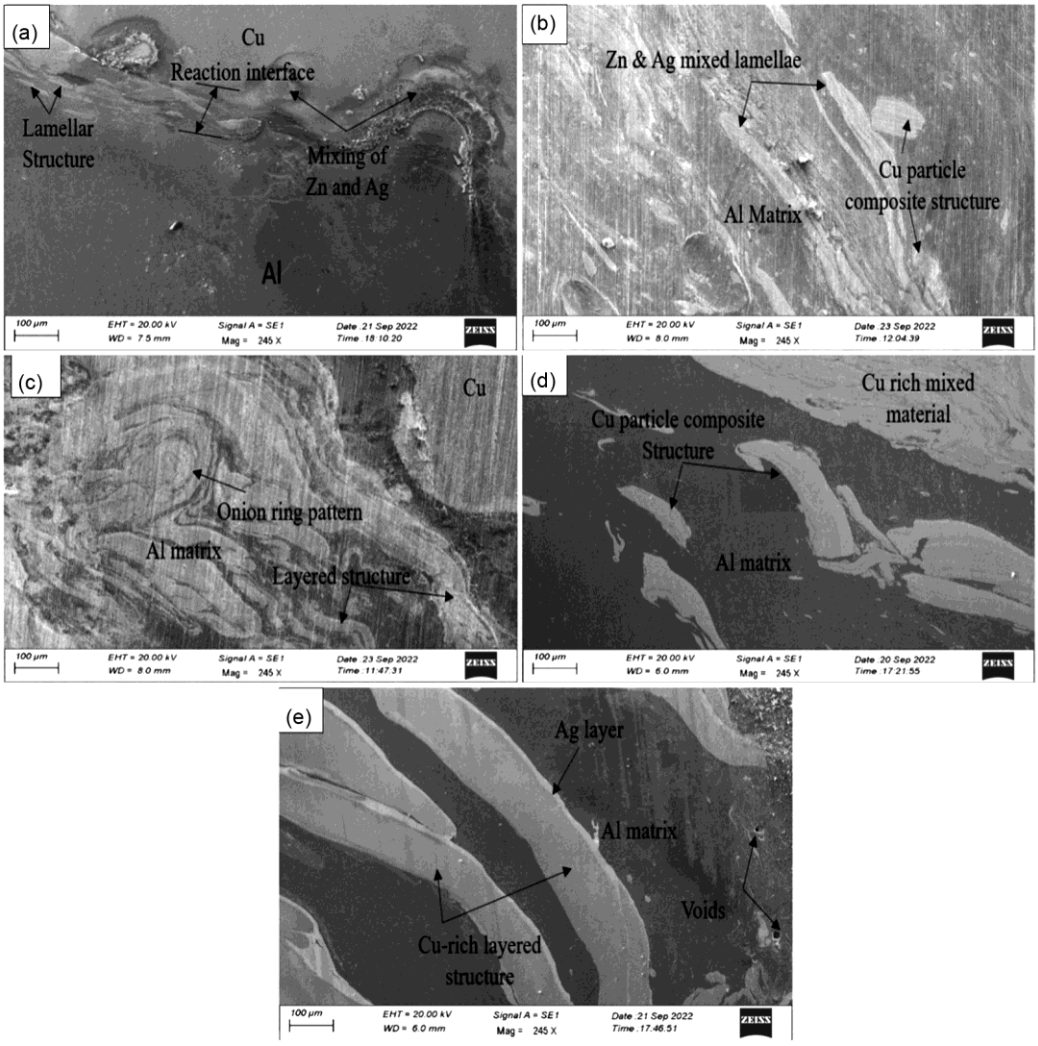

Fig. 5 — Microstructure and SEM image of defect free hybrid interlayer (Ag-Zn) incorporated FSWed Al6101/C11000 joints: (a) J_2, (b) J_6, (c) J_7, (d) J_8, and (e) J_9.

the copper side's edge along the interface exhibited a layered structure (Fig. 5(c)).

The use of mechanical stirring brought on by the rotation of the pin results in the separation of copper fragments from the copper base metal [45]. These detached copper fragments along with the interlayers were deposited in aluminium matrix. This led to the distribution of copper, interlayer fragments, and particles throughout the nugget zone. The formation of intermetallic compounds and metallurgical bonding are aided by the combined influence of frictional heat and heat from plastic deformation, which promotes solid-state interdiffusion and metallurgical reactions between the parent metals and interlayers.

The SEM images are presented in Fig. 5 with a comprehensive overview of defect free Al-Cu joints produced through FSW process at different rotational speeds. Each figure provides unique insights into the quality of the joints and the extent to which the materials have mixed. Figure 5(a) depicts an SEM image of an Al-Cu joint created using FSW at 800 rpm. It is evident that the materials did not mix effectively, leading to a suboptimal result. This poor mixing can be attributed to the fact that there was not enough heat input during the welding process, which is necessary for the aluminium and copper to fuse properly. Fig. 5b showcases an SEM image of an Al-Cu joint produced through FSW at 1000 rpm. The image displays a microstructure characterized by a discontinuous layered pattern that has diffused inconsistently into the aluminium matrix. The presence of this pattern suggests an improved blending of the materials compared to the 800-rpm case. Figure 5(c) presents an SEM image of an Al-Cu joint produced through FSW at 1200 rpm. The image exhibits a distinct microstructure characterized by a continuous layered pattern that has diffused into the aluminium matrix. Notably, the materials have undergone mixing in a manner reminiscent of an "onion ring" pattern. The continuous layered structure diffused within the aluminium matrix indicates a more uniform and integrated blend of the aluminium and copper. The "onion ring" pattern implies that the mixing has occurred in concentric rings or layers, further demonstrating a more intricate and well-incorporated fusion of the materials. Fig. 5(d) displays an SEM image of an Al-Cu joint created through FSW at 1400 rpm. However, the image suggests that the mixing process was not proper, and there are thick copper pieces scattered in a discontinuous manner within the joint. Fig. 5(e) reveals an SEM image of an FSWed Al-Cu joint produced at 1600 rpm. The image depicts a copper-rich layered structure that has diffused within the aluminium matrix. This observation is consistent with the findings of Heideman et al.[46] and Mubiayi et al.[47], who reported similar results. This structure suggests the possibility of more copper rich intermetallic in the stir zone which is not beneficial for good joint strength, emphasizing that further increasing the rotational speed may lower the quality of the joint. This indicates that the rotational speed beyond a certain limit result in poor mixing.

Table 5 illustrates the atomic percentages (at. %) of Al, Cu, Ag, and zinc Zn for different spectrum shown at a specific location in the stir zone of Fig. 6. The results from EDX analysis suggest the possible presence of a phase based on the proportions of Al, Cu, Zn, and Ag.

Figure 6(a) contains an SEM image depicting the stir zone of an Al-Cu joint that has been FSWed with a hybrid interlayer (Ag & Zn) at a processing speed of 1200 rpm. The FSW process causes thermomechanical effects that lead to the melting of the Zn interlayer, resulting in the dispersion of its particles throughout the weld zone. The Energy-Dispersive X-ray Spectroscopy (EDS) analysis conducted afterwards reveals the presence of an interdiffusion region primarily composed of an Al-(Zn) solid solution, as shown in the stir zone of Fig. 6(a), with the related results displayed in Fig. 6(b). Table 5 provides the atomic percentage (at. %) of aluminium (Al), silver (Ag), zinc (Zn), and copper (Cu) at that specific location. This result is consistent with findings reported by Mokabberi et al.[48]. The introduction of molten zinc

Table 5 — EDS analyses for different spectra at a specific location in the stir zone are summarized based on Fig. 6.

Spectrum	Al	Cu	Zn	Ag	Possible phase
	at.%	at.%	at.%	at.%	
1	70.95	1.45	27.49	0.11	Al-(Zn) solid solution
2	51.03	35.82	13.1	0.05	$Al_{4.2}Cu_{3.2}Zn_{0.7}$
3	2.14	35.82	3.22	58.82	(Ag-Cu) rich
4	17.03	67.28	1.07	14.62	Diffusion Layer
5	34.37	0.12	0.13	65.38	Ag_2Al

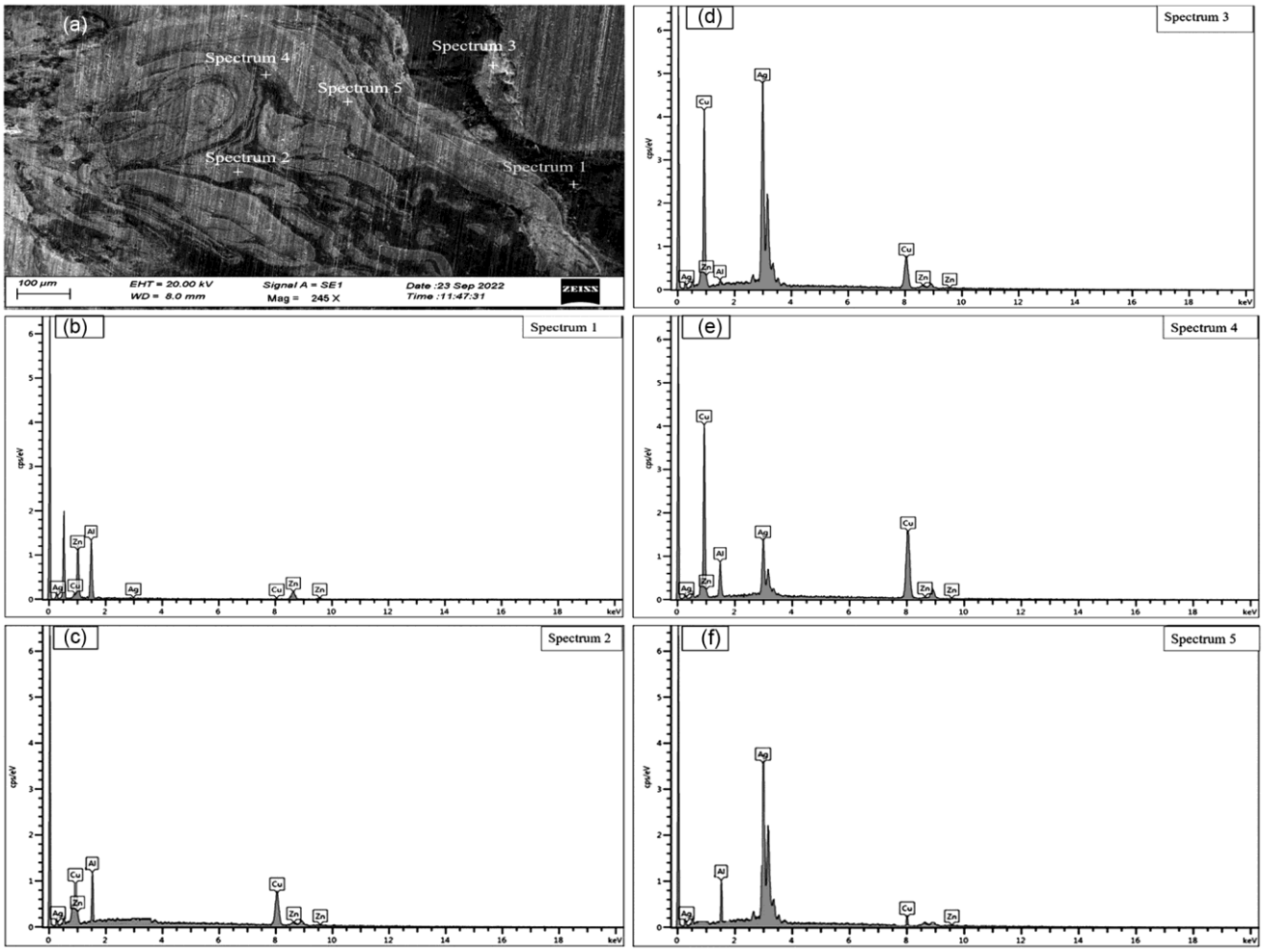

Fig. 6 — The results of FESEM-EDS analysis at different points in the stir zone of FSWed joint J_7: (a) SEM image of Stir zone, (b) represents spectrum 1, (c) represents spectrum 2, (d) represents spectrum 3, (e) represents spectrum 4, and (f) represents spectrum 5.

(Zn) in the Al/Cu interface is recognized for its role in enhancing wettability and initiating a self-propagating reaction, promoting effective bonding [49-51]. The results obtained through EDS analysis confirm a greater equilibrium solubility of aluminium (Al) in Zn within the weld zone in comparison to copper (Cu) in Zn. This dissimilarity leads to the formation of an Al-Zn eutectic composition in the nugget zone, a phenomenon also supported by Shen et al.'s investigations [52], which demonstrate the development of an Al-Zn eutectic structure in Al/Zn/steel joints due to interdiffusion between Al and Zn. The work of Shen et al.[53] further elucidates the liquid–solid reaction mechanism, facilitating the bonding between the inherent Al-Zn layer and the surrounding materials.

Within the observed swirl flow, EDS analysis additionally identifies the presence of the $Al_{4.2}Cu_{3.2}Zn_{0.7}$ IMC at spectrum 2 in stir zone in Fig. 6(a), with the corresponding outcomes illustrated in Fig. 6c (refer to Table 5 for its chemical composition).

The current study has shown that incorporating a zinc (Zn) interlayer can effectively prevent the formation of brittle aluminium-copper (Al_4Cu_9) IMC at the interface of Al and Cu. Instead, it promotes the formation of the ternary $Al_{4.2}Cu_{3.2}Zn_{0.7}$ phase. This phenomenon could be attributed to the chemical affinity between Cu and Zn. The FSW process plays a crucial role in facilitating the Al-Zn-Cu reaction through two primary mechanisms. First, the Zn foil reacts with Cu when it melts owing to its low melting point. Second, aluminium reacts with copper owing to its relatively high electronegativity. This concurrent reaction favoured the formation of a $Al_{4.2}Cu_{3.2}Zn_{0.7}$ ternary phase. Existing research [15, 29-31, 54-56] has demonstrated that the $Al_{4.2}Cu_{3.2}Zn_{0.7}$ ternary phase functions as an effective diffusion

barrier, preventing the formation of detrimental (Al_4Cu_9) IMC.

The presence of the (Ag-Cu) rich layer near the Cu interface at spectrum 3 in stir zone in Fig. 6(a), with the corresponding outcomes illustrated in Fig. 6(d), outlined in Table 5 for its chemical composition, is a result of the mechanical mixing offered by the FSW process. The mechanical stirring promotes the interdiffusion of Ag and Cu, giving rise to the observed (Ag-Cu) rich layer. This mechanical mixing is affirmed by EDS analysis, confirming the existence of Ag and Cu in this mixed layer. The research of Shafiei et al.[57]has been helpful in confirming the findings presented in this study. Their investigation on the formation of intermetallics during furnace brazing of pure titanium to 304 stainless steel using Ag (30–50%)-Cu filler metals revealed the presence of an Ag-Cu rich phase. In essence, FSW's mechanical actions during welding bring about the creation of this unique layer, facilitated by a combination of heat, plastic deformation, and vigorous stirring. Spectrum 4 of Fig. 6(a), near the swirl flow in stir zone, with the corresponding outcomes illustrated in Fig. 6(e) confirms the presence of diffusion layer. FSW generates heat, stirring materials and leading to their amalgamation into a distinct layer. Similarly, Shujin et al.[23] documented the identification of a diffusion layer with a composition of 41.70% aluminium (Al), 48.28% copper (Cu), and 10.02% zinc (Zn) by atom percentage.

EDS analysis was employed to examine spectrum 5, denoted in stir zone in Fig. 6(a), with the corresponding outcomes illustrated in Fig. 6(f). Table 5 provides the atomic percentage (at. %) of aluminium (Al), silver (Ag), zinc (Zn), and copper (Cu) at that specific location. The elemental ratios obtained from the EDS data indicate a potential chemical composition corresponding to IMC Ag_2Al. These observations align with prior research findings as reported by various investigators [28, 31, 58, 59]. Pratap et al.[60] examined the temperature distribution across various trials during the FSW of Al6101/C11000 joints within the weld line region. The plates, characterized by a thickness of 5 mm, were subjected to FSW using a square pin profile tool made of hardened H13 steel. Notably, the investigation revealed that the highest temperature 293°C was identified within the joint area under conditions involving a tool rotational speed of 1200 rpm, a welding speed of 20 mm/min. Shao et al. conducted a study investigating the formation of intermetallic compounds (IMCs) in the Ag-Al system. The findings indicated that at 200°C under solid-state reaction conditions, the atomic diffusion of Ag and Al led to the development of δ-Ag_2Al and μ-Ag_3Al at the joint interface [58]. Our current research has also identified the formation of Ag_2Al intermetallics.

It is noteworthy that, contrary to findings in other research endeavours [13, 61-63], the present study incorporating the Ag & Zn as hybrid interlayer did not observe the presence of brittle intermetallic compounds such as AlCu,Al_4Cu_3,Al_2Cu_3 and $AlCu_3$. The use of a hybrid interlayer (Ag and Zn) during the FSW process is effective in preventing brittle IMCs related to Al-Cu and helps enhance the material properties at the Al/Cu interface.

Figure 7(a) provides a visual representation of the weld nugget morphologies in joint J_7 through elemental mapping. The Royal Blue color indicates aluminum, red represents copper, sky blue stands for silver, and green signifies zinc. The distributions of Zn and Ag in the nugget zone are depicted in Fig. 7(b), showing their consistent diffusion. Notably, a thin layer of Ag is visible in its individual distribution. Within the

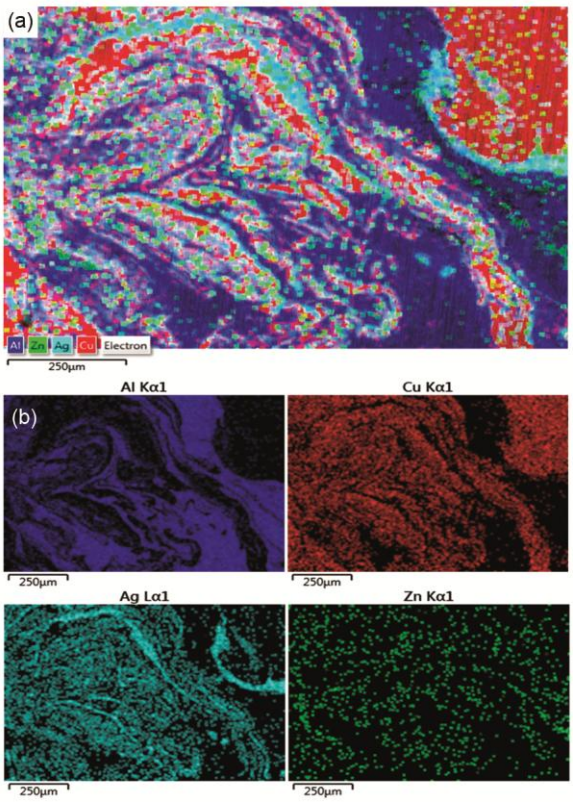

Fig. 7 — Element distribution mapping of FSWed joint J_7: (a) overall mapping, and (b) Al, Cu, Ag and Zn individually.

aluminium matrix, Fig. 7(a) depicts intercalated layers of Cu, Ag, and Zn, resembling wave-like structures observed in previous studies[31, 64].

During friction stir welding, zinc experiences significant deformation owing to its low melting point. Instead of completely melting, it partially melts in certain areas, resulting in the creation of a mixed zone between the layers of aluminium, copper, silver, and zinc. This partial melting triggers the creation of various intermetallics of Al-Cu, Cu-Zn, Al-Zn, Ag-Zn, Al-Ag, and Cu-Ag, depending on the dominant conditions. The significantly deformed Zn layer, merges with the other layers during the stirring process of FSW. This blending process plays a crucial role in the formation of these intermetallics, as evidenced by the findings of other studies [31, 65-71]. Owing to substantial plastic deformation, the interface between the parent material and interlayers may give rise to the formation of several IMCs, including $AlCu$,Al_2Cu, Ag_2Al,Ag_3Al,$AgZn_3$,$Al_{4.2}Cu_{3.2}Zn_{0.7}$, Cu_5Zn_8 and $CuZn_5$[31], through the process of diffusion. However, according to the EDX analysis, in the case of joint J_7, Al–(Zn) solid solution $Al_{4.2}Cu_{3.2}Zn_{0.7}$, Ag_2Al, (Ag-Cu) rich phase, and a diffusion layer was formed.

3.3 Tensile properties

Achieving sound tensile strength in FSW requires a delicate balance between tool traverse speed and rotational speed. This balance affects heat input, material softening, mixing, joint formation, and microstructural characteristics, all of which contribute to the overall performance of the joint.

Figure 8 shows the ultimate tensile strength (UTM) of the FSW-welded Al/Cu joints with a hybrid interlayer (Ag and Zn). The study explores different tool traverse speeds—0.75 mm/sec, 1.25 mm/sec, and 2.25 mm/sec—while keeping a constant rotational speed of 800 rpm and a tilt angle of 2°. At the lower traverse speed (0.75 mm/sec), the joints exhibit a moderate tensile strength of 101.43±8.87 MPa, constituting approximately 51.48% of the Al base metal strength. Conversely, at a traverse speed of 1.25 mm/sec, the joints demonstrated an increased tensile strength of 119.52±11.2 MPa, equivalent to approximately 60.67% of the Al base metal strength. Meanwhile, at a traverse speed of 2.25 mm/sec, the joints displayed a reduced tensile strength of 37.3±10.34 MPa, representing approximately 18.93% of the Al base metal strength.

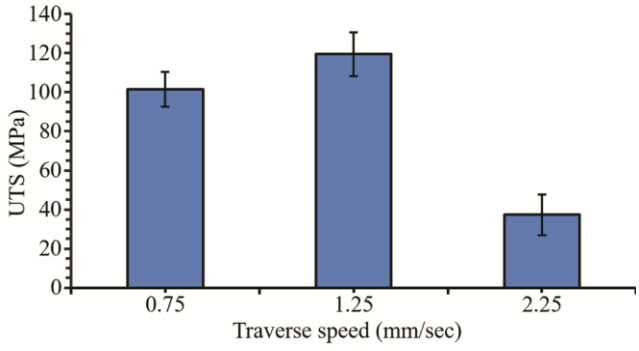

Fig. 8 — Variation of joint strength with traverse speed.

The tensile strength observed at the lower traverse speed of 0.75 mm/sec is relatively moderate, possibly due to the formation of a thicker layer of IMCs at the Al/Cu interface. This thicker IMCs layer, while making the interface more brittle, played a crucial role in the initiation and spread of cracks during loading. Consequently, the strength of the joints is negatively affected. The increase in IMCs layer thickness at lower traverse speeds compromises the overall mechanical properties of the welded joints. The thicker layer of IMCs makes the joints more brittle, leading to an increased likelihood of cracks forming and spreading when the joints are under tension. This observed impact is consistent with the results obtained in earlier investigations[33, 44, 63, 72], which have likewise highlighted the adverse effects of thicker IMCs layers on the mechanical behaviour of friction-stir-welded joints.

As the traverse speed increased to 1.25 mm/sec, there was a gradual improvement in the tensile strength, reaching a value of 119.52±11.2 MPa. The enhancement in the tensile strength can be associated with the formation of a consistent and thin layer of IMCs at the Al/Cu interface. This thin layer acts as a barrier, making it more challenging for cracks to initiate and propagate. Therefore, careful management of the IMC formation is important for improving the mechanical properties of FSW Al/Cu joints[44].

The tensile strength increased as the traverse speed increased from the lowest to moderate level. However, at the highest traverse speed of 2.25 mm/sec, the tensile strength drops to a minimum value of 37.3±10.34 MPa. The effective mixing of materials in the NZ results in the formation of a distinct interface layer, providing a base for the generation of IMCs. According to the studies of researchers W. Zhang [73] and D. Yaduwanshi [74], the rate at which IMCs form at the interface is controlled by the diffusion of materials into each other. This phenomenon is intricately linked to the time and

temperature. The tool's limited interaction time and inadequate plasticization at the highest traverse speed hinder the proper diffusion of materials (Al, Ag, Zn, Cu), as highlighted in Table 4 for jointJ_5. However, indications exist for copper to flow into aluminum at the highest traverse speed, implying the accumulation of a mixture of Al and Cu at the interface. Moreover, the extended interaction time between the tool and workpiece at the lowest traverse speed facilitates sufficient time and heat for a more intensive material diffusion. Consequently, this leads to an increase in the thickness of the interface layer, which decreases with an increase in the traverse speed [75].

Ouyang et al.[17] noted the occurrence of brittle IMCs during direct FSW of 6061 Al/Cu. The formation of IMCs was found to be influenced by the heat input generated by tool rotation. Fig. 9 shows the common locations and surfaces where tensile fractures occurred in the Al/Cu joints fabricated using various parameters (Table 3).

Figure 10 illustrates the ultimate tensile strength (UTM) of FSWed Al/Cu joints, incorporating a hybrid interlayer (Ag & Zn), considering various tool rotational speeds (800, 1000, 1200, 1400, 1600, and 1800 rpm) while maintaining a constant traverse speed of 1.25 mm/sec and a tilt angle of 2°. The results show that strength increases from 800 to 1200 rpm as sufficient frictional heat is generated, ensuring proper joint formation. However, as rotational speed continues to rise beyond this range, these characteristics start to decrease.

An increase in rotational speed resulted in higher temperature, heating and cooling rates, causing the stir zone to experience comparatively elevated temperatures. The study identified that the joint strength and efficiency were maximum at 1200 rpm, with an average UTS of 156.19±10.08 MPa and joint efficiency of 79.28%, beyond this it diminishes and was 91.92 ±11.55 MPa and 46.66%, respectively at 1800 rpm.

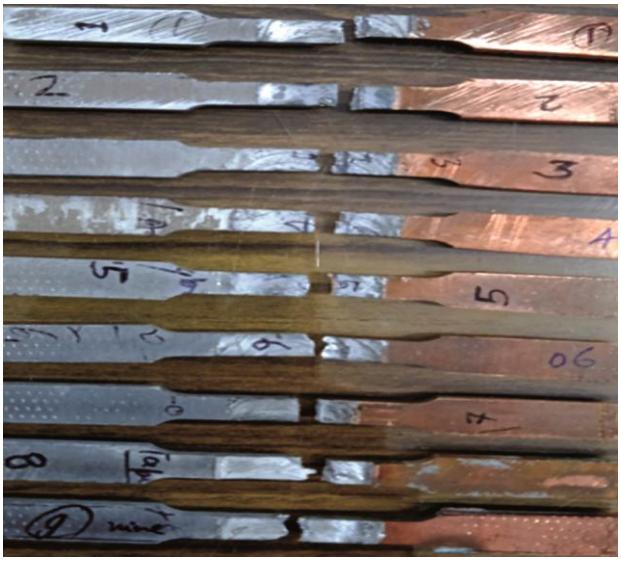

Fig. 9 — Tensile-tested specimen.

Analysis of the microstructure at 1200 rpm showed effective material mixing in the stir zone, creating a dispersed particle arrangement in the aluminium matrix and forming a composite structure. In contrast, at higher rotational speeds, a higher heat input resulted in the development of overlapping IMC layers, leading to rapid crack initiation and a decrease in tensile strength. At a lower rotational speed of 800 rpm, inadequate mixing in the stir zone was observed (Fig. 5(a)), suggesting challenges in the reaction and mixing of the Cu pieces with the Al matrix. This finding is consistent with literature indicating that the weak bonding of Al and Cu at low rotational speeds, potentially leading to defects in the nugget zone [76, 77]. At a moderate rotational speed of 1000 rpm, increased stirring and enhanced friction resulted in higher temperatures in the nugget zone, enabling sufficient reactions between parent metals and interlayers. This led to a defect-free nugget zone and improved joint integrity (Fig. 5(b)).

This study emphasized the role of rotational speed in the formation of IMCs in the weld zone of FSWed Al6101/C11000 joints. Higher rotational speeds increased friction and heat, accelerating atom diffusion and resulting in the formation of thicker IMC layers. This phenomenon impacts the joint's tensile strength, with thicker IMC layers at higher rotational speeds leading to weaker joints.

At the lowest rotational speed of 800 rpm, the IMC layer discontinuously formed with a thin layer at the joint interface (Fig. 5(a)), resulting in a weak metallurgical bond between the intermetallics.

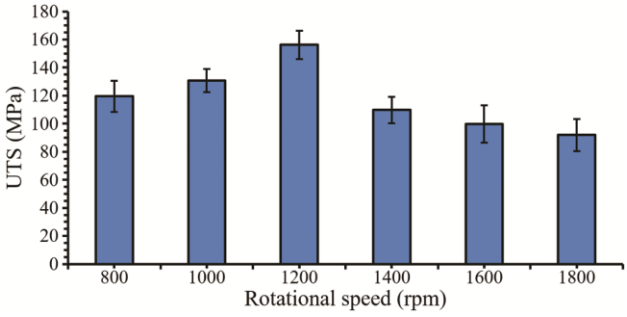

Fig. 10 — Variation of joint strength at different rotational speeds while maintaining a constant traverse speed of 1.25 mm/sec.

Consequently, this reduces the tensile strength of the joint. On the other hand, when a continuous IMC layer with sufficient thickness forms at speeds above 800 rpm, it enhances both the mechanical and metallurgical bonding in the weld zone, consequently improving the tensile properties. Which is consistent with prior research[1, 33, 42, 78], and aligns with findings indicating that joints exhibiting higher tensile properties possess a continuous interfacial IMC layer with an appropriate thickness.

The nugget zone exhibits a sound weld surface at a rotational speed of 1200 rpm (Fig. 6). At 1200 rpm the tensile property is also maximum. Hence, EDX analysis was performed at this speed to determine the cause. Importantly, at a rotation rate of 1200 rpm, the specific characteristics of the Al-Cu IMCs were not prominently visible in the selected areas. Instead, the presence of an Al-(Zn) solid solution, thin and uniform diffusion layer, binary-phase Ag_2Al, and ternary-phase $Al_{4.2}Cu_{3.2}Zn_{0.7}$ was observed in the stir zone/weld zone of the joint. It contributes to the highest tensile strength of 156.19±10.08 MPa, surpassing that of other joints produced in this study. Previous studies have pointed out that achieving the best tensile strength in joints requires effective diffusion[79], prevention of brittle IMCs[80], and establishment of a solid solution phase for constitutional strengthening [72, 81]. Other researchers identified similar strengthening effects [79, 80]. The joint improvement in tensile strength was significantly influenced by the combined effect of the composite-like structure, fine grains in the stir zone, and Orowan strengthening effect [82] caused by dispersed IMCs.

The creation of brittle and hard IMC layers in the FSW process, especially when dealing with dissimilar Al alloys and Cu, is a critical factor that significantly affects the mechanical properties of joints[83]. In these situations, when copper (Cu) pieces detach from the Cu alloy and disperse within the aluminium (Al) matrix along with the Zn and Ag interlayers, IMC formation occurs through solid-state diffusion in the stir zone. Xue et al.[84] explored the impact of welding parameters on joint strength and revealed that achieving a sound joint requires the dispersion of a thin and continuous layer in the weld area. Notably, the thickness of the IMCs in the FSW process tends to increase with higher rotational speeds owing to the enhanced interaction between the Al and Cu materials.

Ensuring the correct thickness of the joint is closely tied to maintaining proper fluidity and stirring in the weld zone. This ensured optimal bonding of the weld layer to the Al–Cu materials, facilitating the effective diffusion of aluminium (Al), silver (Ag), zinc (Zn), and copper (Cu) atoms at the joint interfaces. This process contributes to the formation of strong metallurgical joints between Al and Cu. At higher rotation rates, the pin's mixing action became more pronounced, leading to a greater number of copper pieces being moved towards the aluminium side. This resulted in the observation of a significant Cu-rich layer at the Al–Cu interface at high rotation speeds Fig. 5 (d & e).

The bonding conditions at the interface of the Al and Cu were significantly affected by the rotational rate, as illustrated in Fig. 5. The thickness of the IMC layer increases with higher rotation rates due to enhanced reactions between Al and Cu at high rotational speeds. In addition, layered structures tended to form in the presence of significant amounts of copper near the interface and weld zone Fig. 5(d & e). At higher rotation speeds, copper (Cu) becomes more malleable owing to the increased temperatures, making the stirring action more intense. In these situations, even larger Cu pieces can easily move away from the Cu bulk. Multiple Cu pieces were likely displaced simultaneously, engaging in mixing and reacting with the Al matrix at the interface. This process resulted in the formation of substantially stacked layered structures. Challenges arise when large Cu pieces are close to the interface, hindering the smooth flow of the detached Cu pieces and leading to their accumulation at the interface. Consequently, the development of thick stacked layered structures becomes more prominent, causing a decrease in tensile strength beyond the rotational speed of 1200 rpm.

3.3 Fracture behaviour

The examination of optimal tensile strength at a rotational speed of 1200 rpm prompted a focused fractographic analysis utilizing SEM images of joint J_7's fracture surface (Fig. 11). Within this joint, identified phases include the Al-(Zn) solid solution, a thin and uniform diffusion layer, binary-phase Ag_2Al, ternary-phase $Al_{4.2}Cu_{3.2}Zn_{0.7}$, and an Ag-Cu-rich phase (Fig. 6). Notably, these phases exhibit reduced brittleness and increased ductility compared to intermetallics formed through the interaction of parent metals Al-Cu, such as Al_2Cu,Al_4Cu_9.

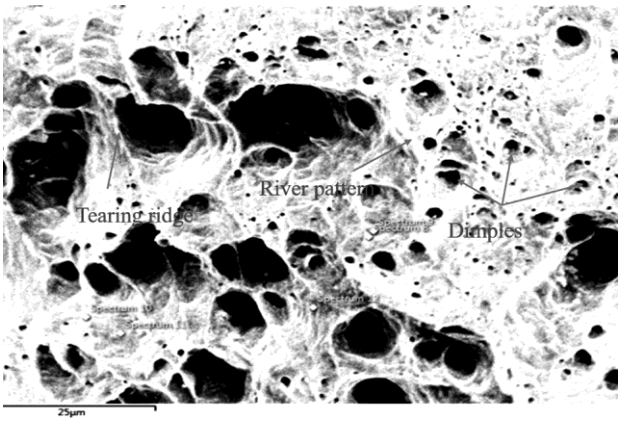

Fig. 11 — Fracture surface of the joint produced 1200 rpm.

The fracture surface of joint J_7 predominantly features dimples of varying sizes, indicative of a ductile fracture mode. The observed formation of deep dimples suggests void expansion within the sample, signifying a substantial energy involvement in the fracture process [85].

The development of brittle IMCs in traditional Al-Cu FSW is a common issue that often leads to reduced ductility and tensile strength. The use of Zn and Ag interlayers has been found to mitigate the negative consequences by facilitating the growth of less harmful intermetallics [31]. This aligns with previous finding reported by researchers [28, 56, 85, 86]. Consequently, the observed reduction in the formation of highly brittle intermetallics likely contributes to the ductile fracture behaviour and the attainment of the highest tensile strength at 1200 rpm in the FSWed joints.

4 Conclusion

In summary, the friction stir welding of Aluminium 6101 and Copper C11000, incorporating a hybrid interlayer (Ag & Zn) at different welding parameters, investigation highlights the pivotal interaction between tool traverse speed and rotational speed for achieving optimal tensile strength. The following key conclusions emerge:

i. Sound joint of Al6101/C11000 with hybrid interlayer (Ag & Zn) was successfully achieved by friction stir welding.

ii. A sound weld surface and highest tensile strength is achieved at 1200 rpm rotational speed and 1.25 mm/ sec traverse speed, emphasizing the importance of proper diffusion, controlled IMC formation, and solid solution phase development in optimizing tensile strength. Cu, Ag and Zn particles consisting of thin and uniform diffusion layer dispersed in the Al matrix to form composite-like structure. The presence of an Al-(Zn) solid solution, thin and uniform diffusion layer, binary-phase Ag_2Al, and ternary-phase $Al_{4.2}Cu_{3.2}Zn_{0.7}$ in the weld zone of the joint contributed to the highest tensile strength of 156.19±10.08 MPa.

iii. Rotational speeds ranging from 800 to 1200 rpm contribute to increased strength through adequate frictional heat generation, promoting effective joint formation. Lower rotational speeds lead to insufficient mixing, indicating challenges in Cu-Al and interlayers diffusion in the nugget zone. The lower rotational speed of 800 rpm results in a discontinuous IMC layer and weak metallurgical bonding, contributing to reduced tensile strength. Beyond 1200 rpm, a diminishing trend in strength is observed, higher speed leads to higher temperature, resulted in thicker IMC layers, impacting the stir zone's mechanical properties.

iv. Fracture surface of the joint formed at 1200 rpm shows dimples of varying sizes, indicating a ductile fracture mode. Incorporation of Zn and Ag interlayers in FSW diminishes highly brittle intermetallics (Al_4Cu_9 andAl_2Cu), promoting less harmful intermetallics (Al-Zn solid solution, $Al_{4.2}Cu_{3.2}Zn_{0.7}$, Ag-Cu rich, Ag_2Al) contributes to observed ductile fracturebehaviour and highest tensile strength.

Acknowledgement

We gratefully acknowledge the financial support provided by the Science and Engineering Research Board (SERB) under grant number CRG/2022/002222, dated July 18, 2023, Department of Science and Technology (DST), Government of India, which made this research possible.

References

1 Bagheri B, Alizadeh M, Mirsalehi SE, Shamsipur A, Abdollahzadeh A,*WeldWorld*, 66(11) (2022) 2333.
2 Mehta K P, Badheka V J, *Trans. Nonferrous Met Soc China*, 27(1) (2017) 36.
3 Ghiasvand A, Hassanifard S, Jalilian M M, Kheradmandan H, *WeldWorld*, 65(3) (2021) 441.
4 Memon S, Paidar M, Mehta KP, Babaei B, Lankarani HM, *JMEPEG*,30(1) (2021) 334.
5 Habibizadeh A, Honarpisheh M, Golabi S, *Weld World*, 66(9) (2022) 1757.
6 Zhang W, Shen Y, Yan Y, Guo R, Guan W, Guo G, *Int J Adv Manuf Technol*, 94(1) (2018) 1021.

7 Zhang C, Shirzadi A A, *Sci Technol Weld Joi*, 23(5) (2018) 394.
8 Li G, Zhou L, Zhou W, Song X, Huang Y, *J Mater Res Technol*, 8(3) (2019) 2613.
9 Akbari M, Abdi Behnagh R, Dadvand A, *Sci Technol Weld Joi*, 17(7) (2012) 581.
10 Regensburg A, Petzoldt F, Benss T, Bergmann J P, *Weld World*, 63(1) (2019) 117.
11 Yang X, Li W, Xu Y, Wen Q, Feng W, Wang Y, *Weld World*, 63(1) (2019) 127.
12 Abbasi M, Givi M, Bagheri B, *Proc IMechE Part B: J Engineering Manufacture*, 0(0) (2020) 1.
13 Tan C W, Jiang Z G, Li L Q, Chen Y B, Chen X Y, *Materials & Design*, 51 (2013) 466.
14 Liu P, Shi Q, Wang W, Wang X, Zhang Z, *Materials letters*, 62(25) (2008) 4106.
15 Boucherit A, Avettand-Fenoel M N, Taillard R, *Materials & Design*, 124 (2017) 87.
16 Avettand-Fenoel M N, Taillard R, Ji G, Goran D, *Metall Mater Trans A*, 43 (2012) 4655.
17 Ouyang J, Yarrapareddy E, Kovacevic R, *J Mater Process Technol*, 172(1) (2006) 110.
18 Elrefaey A, Takahashi M, Ikeuchi K, *Weld World*, 49 (2005) 93.
19 Hou W, Shen Z, Huda N, Oheil M, Shen Y, Jahed H, Gerlich A P, *Materials Science & Engineering A*, 809 (2021) 140992.
20 Sahu P K, Pal S, Pal S K, *Metall Mater Trans A*, 48(7) (2017) 3300.
21 Yarmolenko M V, *Physics and Chemistry of Solid State*, 22(1) (2021) 80.
22 Wang C, Li C, Luo Z, Li M, Lin N, Ding K, Man S, Duan J A, *J Mater Sci: Mater Electron*, 32(14) (2021) 19543.
23 Chen S, Wang D, Li R, Liu B, Wang J, *JMEPEG*, 28 (2019) 5245.
24 Mehta K P, Badheka V J, *Int J Adv Manuf Technol*, 80 (2015) 2073.
25 Liu H J, Shen J J, Zhou L, Zhao YQ, Liu C, Kuang L Y, *Sci Technol Weld Joi*, 16(1) (2011) 92.
26 Chularis A A, Rzaev R A, Syndetov M K, *Welding International*, 34(4-6) (2020) 230.
27 Payak V, Paulraj J, Roy B S, Bhargava M, Das P, *Proc IMechE Part E:J Process Mechanical Engineering*, 238(3) (2023)1462.
28 Pandya S N, Menghani J, *Metall Mater Eng*, 24(1) (2018) 45.
29 Boucherit A, Abdi S, Aissani M, Mehdi B, Abib K, Badji R, *Int J Adv Manuf Technol*, 111 (2020) 1553.
30 Liu H, Zuo Y, Ji S, Dong J, Zhao H, *JMR&T*, 18 (2022) 85.
31 Payak V, Paulraj J, Roy BS, Bhargava M, Choudhury S, *Int J Adv Manuf Tech*, 128(3-4) (2023) 1419.
32 Sahu PK, Pal S, Pal SK, Jain R, *J Mater Process Technol*, 235 (2016) 55.
33 Xue P, Ni D R, Wang D, Xiao B L, Ma Z Y, *Mater Sci Eng A*, 528(13-14) (2011) 4683.
34 Dong F, Chen W, Su G, Zhao X, *Trans China Weld Inst*, (10) (2011) 85.
35 Akinlabi E T, Els-Botes A, McGrath P J,*Proceedings of 2nd IC on AET*, Uganda, (2011).
36 Fotouhi Y, Rasaee S, Askari A, Bisadi H, *Eng Solid Mech*, 2(3) (2014) 239.
37 Muthu, M.F.X. and V. Jayabalan, *J Mater Process Technol*, 217 (2015) 105.
38 Zhang C, Cao Y, Huang G, Zeng Q, Zhu Y, Huang X, Li N, Liu Q,*J Manuf Process*, 49 (2020) 214.
39 Galvao I, Loureiro A, Rodrigues D M, *Sci Technol Weld Joi*, 21(7) (2016) 523.
40 Muhammad NA, Wu C, *Int J Mech Sci*, 183 (2020) 105784.
41 Galvao I, Leal R M, Loureiro A, Rodrigues D M, *Sci Technol Weld Joi*, 15(8) (2010) 654.
42 Galvao I, Oliveira J C, Loureiro A, Rodrigues D M, *Sci Technol Weld Joi*, 16(8) (2011) 681.
43 Hou W, Shah L H, Huang G, Shen Y, Gerlich A, *J Alloys Compd*, 825 (2020) 154045.
44 Mao Y, Ni Y, Xiao X, Qin D, Fu L, *J Manuf Process*, 60 (2020) 356.
45 Mehta K P, Badheka V J, *Mater Manuf Process*, 31(3) (2016) 233.
46 4Heideman R, Johnson C, Kou S, *Sci Technol Weld Joi*, 15(7) (2010) 597.
47 Mubiayi M P, Akinlabi E T, *Trans Nonferrous Met Soc China*, 26(7) (2016) 1852.
48 Mokabberi S R, Movahedi M, Kokabi A H, *Mater Sci Eng A*, 727 (2018) 1.
49 Tong L, Xie J, Liu L, Chang G, Ojo O O, *JMR&T*, 9(6) (2020) 13239.
50 Paidar M, Ali K A, Mohanavel V, Mehrez S, Ravichandran M, Ojo O O, *Vacuum*, 187 (2021) 110080.
51 Paidar M, Memon S, Samusenkov V O, Babaei B, Ojo O O, *Materials Letters*, 285 (2021) 129160.
52 Shen Z, Chen J, Ding Y, Hou J, Shalchi Amirkhiz B, Chan K, Gerlich A P, *Sci Technol Weld Joi*, 23(6) (2018) 462.
53 Shen Z, Ding Y, Chen J, Amirkhiz BS, Wen J Z, Fu L, Gerlich A P, *J Mater Sci Technol*, 35(6) (2019) 1027.
54 Zhang J, Shen Y, Yao X, X u H, Li B, *Materials & Design*, 64 (2014) 74.
55 Sahu P K, Pal S, Pal S K, *Metall Mater Trans A*, 48 (2017) 3300.
56 Balasundaram R, Patel V K, Bhole S D, Chen D L, *Mater Sci Eng A*, 607 (2014) 277.
57 Shafiei A, Abachi P, Dehghani K, Pourazarang K, *Mater Manuf Process*, 25(11) (2010) 1333.
58 Fu S W, Lee C C, *J Mater Sci: Mater Electron*, 29 (2018) 3985.
59 Fedorov V, Uhlig T, Podlesak H, Wagner G, *Metals*, 10(12) (2020) 1563.
60 Pratap K J, Raj A, Venkatraman A R, Kulandaivel A, Ashwin P G, Narendranathan S K, Ashok N, *Adv Mater Sci Eng*, 2022(1) (2022) 4973839.
61 Abbasi M, Taheri A K, Salehi M T, *J Alloys Compd*, 319(1-2) (2001) 233.
62 Shiraly M, Shamanian M, Toroghinejad M R, Ahmadi Jazani M, *J Mater Eng Perform*, 23 (2014) 413.
63 Abdollah-Zadeh A, Saeid T, Sazgari B, *J Alloys Compd*, 460(1-2) (2008) 535.
64 Muhammad N A, Wu C S, *J Manuf Process*, 39 (2019) 114.
65 Liu H, Ma L, Gong P, Dong J, Yue Y, *T Indian I Metals*, 76(4) (2023) 979.
66 Gao P, Zhang Y, Mehta K P, *Metals and Materials International*, 27 (2021) 3085.
67 Avettand-Fenoel MN, Nagaoka T, Marinova M, Taillard R,*J Manuf Process*, 58(2020)259.
68 Bagheri B, Vaneghi AH, Shamsipur A, Mirsalehi SE, *Research Square* (2022).

69 Li C, Ao S, Wang A, Wei Q, Wu M, Luo Z, *Trans Tianjin Univ*, 26(2020) 305.
70 Anbukkarasi R, Kailas SV, *T Indian I Metals*, 72(2019) 1603.
71 Khajeh R, Jafarian HR, Jabraeili R, Eivani AR, Seyedein SH, Park N, Heidarzadeh A, *JMR&T*, 16(2022) 251.
72 Al-Roubaiy AO, Nabat SM, Batako AD, *Int J Adv ManufTech*, 71(2014) 1631.
73 Zhang W, Shen Y, Yan Y, Guo R, Guan W, Guo G, *Int J Adv Manuf Tech*, 94(2018)1021.
74 Yaduwanshi DK, Bag S, Pal S, *Mater Manuf Process*, 33(3)(2018) 277.
75 Medhi T, Yadava MK, Roy BS, Saha SC, *Int J Adv Manuf Tech*, 104 (2019) 1461.
76 Saeid T, Abdollah-Zadeh AA, Sazgari B, *J Alloys Compd*, 490(1-2)(2010) 652.
77 Watanabe T, Takayama H, Yanagisawa A, *J Mater Process Technol*, 178(1-3) (2006) 342.
78 Sahu PK, Pal S, Shi Q, *SN Applied Sciences*, 1(2019) 1.
79 Xue P, Xiao BL, Ni DR, Ma ZY, *Mater Sci Eng A*, 527 (21-22) (2010) 5723.
80 Kandasamy J, Hussain MM, Rajesham S, *Mater Manuf Process*, 27(12)(2012) 1429.
81 Zhang J, Luo G, Wang Y, Xiao Y, Shen Q, Zhang L, *J Alloys Compd*, 556(2013) 139.
82 Hsu CJ, Chang CY, Kao PW, Ho NJ, Chang CP, *Acta Materialia*, 54(19)(2006) 5241.
83 Muhammad NA, Wu CS, Tian W, *J Alloys Compd*, 785(2019) 512.
84 Xue P, Xiao BA, Ma ZY, *Metall Mater Trans A*, 46(2015) 3091.
85 Regensburg A, Petzoldt F, Benss T, Bergmann JP, *Weld World*, 63(2019) 117.
86 Paidar M, Mohanavel V, Ojo OO, Mehrez S, Rajkumar S, *Results in Physics*, 24(2021) 104101.